Journal of Engineering Physics and Thermophysics, Vol. 78, No. 3, 2005

HEAT AND MASS TRANSFER IN DISPERSE SYSTEMS

INVESTIGATION OF THE MAGNETOPHORETIC PROPERTIES OF LOW-MAGNETIC MICROPARTICLES

B. É. Kashevskii, S. B. Kashevskii, and I. V. Prokhorov

UDC 621.314

A procedure of magnetophoretic investigation of low-magnetic microparticles sedimenting in a fluid under the action of the inhomogeneous magnetic field of two saturation-magnetizable rectangular ferromagnetic rods has been substantiated theoretically. The results of experimental investigation of the magnetic susceptibility of micrometer para- and diamagnetic particles have been presented.

Introduction. In the mid-1970s, the method of magnetic separation attracted attention in many spheres of activity, including water purification and gas scrubbing, clay cleaning, chemical technologies, medicine, and biology [1–7]. Using a magnetic field combining a high strength and a strong small-scale inhomogeneity, one can isolate even very small low-magnetic objects, including particles of cellular suspensions from a gas or fluid flow. High-gradient magnetic filters are traditionally created by application of a homogeneous magnetic field to a volume in which small ferromagnetic bodies are distributed. The finer the particles isolated and the weaker their magnetic properties, the stronger must be the external field and the smaller the dimensions of the elements of a ferromagnetic head. Thus, to isolate red blood cells one uses bundles of ferromagnetic wire about 100 μm in diameter [2, 5]. In flow systems, the efficiency of such a filter structure is low, since the probability of the particle being captured is low and decreases with increase in the pumping rate. Fundamentally new possibilities are offered by the concept of high-gradient magnetic separation on coherent (ordered) magnetic structures [8–11]. The order of a magnetic structure creates prerequisities for a sharp improvement in the properties of a filter by accumulation of the effect of magnetophoretic displacement of the particles isolated in the process of motion of the suspension. Furthermore, periodic structures allow detailed description of the distribution of a magnetic field in them, thus offering possibilities of using mathematical optimization methods. Practical development of an optimum system requires, among other things, data on the magnetic properties of the particles being separated. In many cases, particularly when we are dealing with cellular suspensions, this information is lacking. In such a situation, to measure the magnetic susceptibility of particles, one can use magnetophoretic experiments in which the susceptibility is determined from the particle velocity in a prescribed inhomogeneous field, usually in the field of a ferromagnetic cylinder [12]. Measurements in the cylinder's field are rather difficult, since the particle moves in three directions. In the present work, we have considered and used in practice a more practical magnetophoretic procedure for studying the susceptibility of dia- and paramagnetic microparticles.

Theoretical Prerequisites. The geometry of the magnetophoretic cell in question is shown in Fig. 1. The cell (Fig. 1a) includes a vertical rectangular channel 1 whose horizontal cross section has width $2W$ and length $2L$ ($L >> W$) and two identical rectangular ferrocylinders 2 and 3 of length $2L$, width B, and height $2C$. The direction of observation is indicated by arrow 4. The microscopy zone 5 and the direction of application of the homogeneous external field **H** are shown in Fig. 1b. The channel is filled with a suspension of the particles under study 6 (Fig. 1b), which settle under gravity and arrive at the zone of action of an inhomogeneous field of magnetized cylinders. The origin of the Cartesian coordinate system X, Y, Z is located at the center of the channel between the cylinders (Fig. 1b).

A. V. Luikov Heat and Mass Transfer Institute, National Academy of Sciences of Belarus, 15 P. Brovka Str., Minsk, 220072, Belarus. Translated from Inzhenerno-Fizicheskii Zhurnal, Vol. 78, No. 3, pp. 38–43, May–June, 2005. Original article submitted July 12, 2004.

1062-0125/05/7803-0449

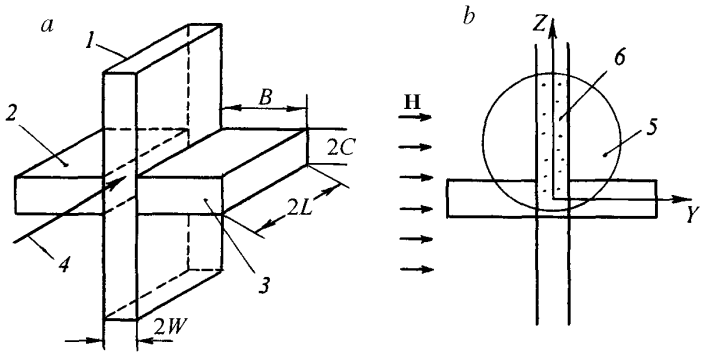

Fig. 1. Geometry of a magnetophoretic cell.

At first sight, selection of such a system may seem unjustified, since the distributions of the magnetic field and the magnetophoretic force in it have a three-dimensional structure. However, by virtue of the system's symmetry, both horizontal components of the magnetophoretic force disappear on the *Y* axis. Observing the vertical movement of the particles in the vicinity of the above axis, we may exclude the influence of transverse forces. In practice, the deflection of a particle from the symmetry plane $Y = 0$ is easily recorded by direct observation. As far as movements in the direction of observation (along the *X* axis) are concerned, we can monitor them by the change in sharpness of the picture.

The equation of motion of a particle in the inertialess approximation is found from the condition of mutual compensation of the sedimentation, viscous, and magnetophoretic forces. On condition that the particle size is small as compared to the inhomogeneity scale of the field, the magnetophoretic force is determined according to [8]

$$\mathbf{F}_{\mathrm{m}} = \frac{1}{2}\Delta\chi V \nabla \mathbf{H}^2 = -\nabla\Phi\,, \quad \Phi = -\frac{1}{2}\Delta\chi V (2\pi I_{\mathrm{s}})^2 [\mathbf{h}^2 + P(\mathbf{eh})]\,, \quad P = \frac{H_0}{\pi I_{\mathrm{s}}}\,. \tag{1}$$

Here $\Delta\chi = \chi - \chi_0$ and $\mathbf{h} = \mathbf{H}'/(2\pi I_{\mathrm{s}})$. Using the quantity $\Phi^* = 2\Delta\chi V(\pi I_{\mathrm{s}})^2$ as the scale of magnetophoretic potential and $|\Phi^*|/W$ as the scale of magnetophoretic force, we rewrite relations (1) in dimensionless form:

$$\varphi = -\mathbf{h}^2 - P(\mathbf{eh})\,, \quad \mathbf{f}_{\mathrm{m}} = -\mathrm{sign}\,(\Delta\chi)\,\nabla\varphi\,. \tag{2}$$

It is noteworthy that the dimensionless potential φ in (2) has been determined for paramagnetic particles ($\Delta\chi > 0$), i.e., paramagnetic particles move in the direction of the φ medium, whereas diamagnetic ones move in the direction of the maximum. Using the Stokes approximation for the viscous force, we represent the equation sought in the form

$$3\alpha\pi d\eta \frac{d\mathbf{R}}{dt} + \mathrm{sign}\,(\Delta\chi)\frac{2|\Delta\chi|\,V(\pi I_{\mathrm{s}})^2}{w}\nabla\varphi + \Delta\rho g V\mathbf{k} = 0\,. \tag{3}$$

Apart from scale of the distance *W*, we introduce the rate scale — the rate of free sedimentation of a particle $v_0 = |\Delta\rho|\,gd^2/18\alpha\eta$. Equation (3) for the dimensionless rate $\boldsymbol{\omega} = v_0^{-1}d\mathbf{R}/dt$ will be written as follows:

$$\boldsymbol{\omega} = -\mathrm{sign}\,(\Delta\rho)\,\mathbf{k} - \mathrm{sign}\,(\Delta\chi)\,M\nabla\varphi\,, \quad M = \frac{2|\Delta\chi|\,\pi^2 I_{\mathrm{s}}^2}{W|\Delta\rho|g}\,. \tag{4}$$

We compute the magnetic field in the system. The cylinders are assumed to be uniformly magnetized to saturation. We note that the field of two cylinders with a gap is equal to the difference of the fields of two imaginary cylinders — a solid cylinder and that filling the gap. Let $A_0(X_0, Y_0, Z_0)$ be a point belonging to the cylinder. The strength of the field created at the point $A(X, Y, Z)$ by an infinitesimal volume $dX_0dY_0dZ_0$ (constructed at the point A_0) is determined by the relation

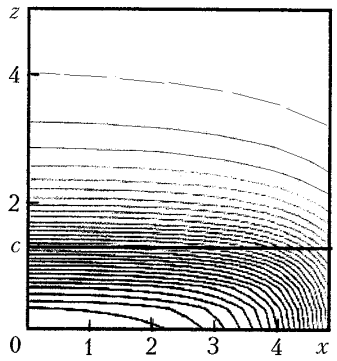

Fig. 2. Isolines of the dimensionless magnetophoretic potential in the channel in the plane $y = 0$.

$$d\mathbf{H}'(\mathrm{A}_0, \mathrm{A}) = -I_s \mathbf{K}(\mathrm{A}_0, \mathrm{A})\, dx_0 dy_0 dz_0 ,$$

where

$$\mathbf{K}(\mathrm{A}_0, \mathrm{A}) = \frac{1}{r^3_{\mathrm{A}_0\mathrm{A}}}\left[\mathbf{e} - 3\frac{(\mathbf{er}_{\mathrm{A}_0\mathrm{A}})\,\mathbf{r}_{\mathrm{A}_0\mathrm{A}}}{r^2_{\mathrm{A}_0\mathrm{A}}}\right]; \quad \mathbf{r}_{\mathrm{A}_0\mathrm{A}} = (x - x_0)\,\mathbf{i} + (y - y_0)\,\mathbf{j} + (z - z_0)\,\mathbf{k}; \quad \mathbf{e} = \frac{\mathbf{H}_0}{H_0}.$$

Here and in what follows, the distances are measured in units of the channel half-width W. In magnetization along y, we obtain

$$K_x = \frac{-3}{r^5}(y - y_0)(x - x_0), \quad K_y = \frac{1}{r^3}\left[1 - 3\frac{(y - y_0)^2}{r^2}\right], \quad K_z = \frac{-3}{r^5}(y - y_0)(z - z_0).$$

The magnetic eigenfield of a rectangular cylinder with the origin of coordinates at the geometric center and sides $2l$, 2β, and $2c$ along the x, y, and z axes is determined by the relation

$$H_i'(x, y, z, l, \beta, c) = -I_s \int_{-c}^{c}\int_{-\beta}^{\beta}\int_{-l}^{l} K_i^{\perp}\, dx_0 dy_0 dz_0 . \qquad (5)$$

We represent the dimensionless-strength components x and z in analytical form:

$$h_x(x, y, z, l, b, c) = \frac{1}{2\pi}[D(x, y, z, l, b + 1, c) - D(x, y, z, l, 1, c)],$$

$$h_z(x, y, z, l, b, c) = \frac{1}{2\pi}[D(z, y, x, l, b + 1, c) - D(z, y, x, l, 1, c)],$$

where

$$D(f, g, h, \alpha, \beta, \gamma) = \ln\frac{F(f, g, h, -\alpha, -\beta, -\gamma)\,F(f, g, h, \alpha, \beta, -\gamma)\,F(f, g, h, \alpha, -\beta, \gamma)\,F(f, g, h, -\alpha, \beta, \gamma)}{F(f, g, h, \alpha, -\beta, -\gamma)\,F(f, g, h, -\alpha, \beta, -\gamma)\,F(f, g, h, -\alpha, -\beta, \gamma)\,F(f, g, h, \alpha, \beta, \gamma)};$$

$$F(f, g, h, \alpha, \beta, \gamma) = -\gamma - h + [(f + \alpha)^2 + (g + \beta)^2 + (h + \gamma)^2]^{1/2}.$$

The expression for the z component is too cumbersome and is not written. One may also find it by numerical integration of (5).

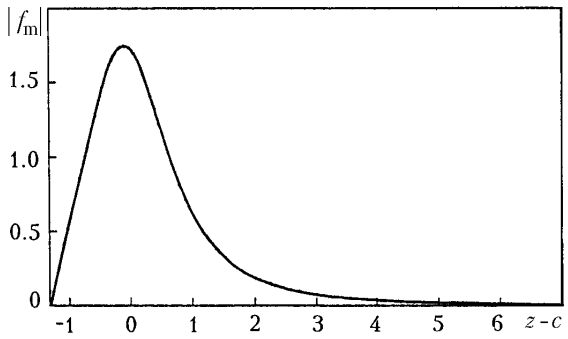

Fig. 3. Change in the absolute value of the dimensionless magnetophoretic force along the z axis.

We consider the distribution of the magnetophoretic potential for conditions that have been realized in the experimental cell described below: W = 0.155 mm, L = 0.75 mm, B = 2 mm, and C = 0.2 mm. The strength of the external field is H_0 = 9100 Oe. We take the value I_s = 1700 G for the saturation magnetization of magnetic cylinders manufactured from transformer steel. Here, P = 1.7. The potential distribution $\varphi(x, z)$ in the plane y = 0 is shown in Fig. 2 by constant-level lines. The difference in values between neighboring lines is 0.1. The change in the absolute value of the dimensionless magnetophoretic force along the z axis is presented in Fig. 3. The absolute value of the force is maximum in the vicinity of the section of the magnetic cylinders.

Experimental Investigation. The experimental cell is a U-shaped channel manufactured by laser cutting from sheet acrylic plastic of thickness 1.3 mm and glued with optical glass on both sides. The measuring arm of the channel has been described above (see Fig. 1). The suspension under study is supplied to the cell via the second arm of width 1.5 mm. The cell is placed in a homogeneous magnetic field, as shown in Fig. 1b. The settling of particles is recorded using a microscope and a digital camera with connection to a personal computer. The distance from the particle to the section of the magnetic cylinders as a function of time is determined on a successive series of frames.

In the first experiment, we have used a suspension of paramagnetic titanium particles in distilled water; the particles were obtained by electrochemical deposition at the Science and Production Powder-Metallurgy Association (Minsk). The result of measurements for a particle about 10 μm in size is presented in Fig. 4 in the coordinates "dimensionless distance to the upper section of ferrocylinders–observation time." It is noteworthy that, at a distance from the cylinders smaller than the channel width, the velocity of the particle increases so that it is impossible to accurately record its position with a frequency of 30 frames per second using a video camera. We compare the result obtained and theory. According to (4), the observation time and the change in the position of the particle in motion along the z axis are related by

$$t = \frac{W}{v_0} D(z, z_0, M), \quad D(z, z_0, M) = -\int_{z_0}^{z} \frac{d\zeta}{\text{sign}(\Delta\rho) + \text{sign}(\Delta\chi)\, M\, (\partial\varphi/\partial\zeta)}, \tag{6}$$

where z_0 is the initial position of the particle and z is the position of the particle at the instant of time t. In the case where a paramagnetic particle is heavier than water, we have sign $(\Delta\rho)$ = sign $(\Delta\chi)$ = 1. We compare dependence (6) and experiment, using the above value W = 155 μm and the value of the dimensionless coordinate that has been measured at the initial instant of recording, $z_0 = c + 5.51$. Next, taking into account the values of the density and magnetic susceptibility of titanium, ρ = 4.5 g/cm^3 and $\chi = 14.4 \cdot 10^{-6}$, and of water, ρ_0 = 1 g/cm^3 and $\chi_0 = -0.72 \cdot 10^{-6}$, and the value of the saturation magnetization of iron $I_s = 1.7 \cdot 10^3$ G, we find M = 16.2. The free-settling rate v_0 is considered as the free (adjustable) parameter. It is impossible to directly measure v_0 with the required accuracy, since the magnetic field exerts a pronounced influence on particle motion at the boundary of the microscopy region. The computation result is presented by curve 1 in Fig. 4 for the above values of z_0 and M and for v_0 = 65 μm/sec. It is seen that, as the magnetic cylinders are approached, a pronounced disagreement occurs between the measured and calculated data. This disagreement can be minimized by selection of the value of M. Thus, curve 2 in Fig. 4 represents a result of calculation for M = 15. This value of M corresponds to the magnetic susceptibility of particles $\chi = 13.28 \cdot 10^{-6}$, which is 7.8% lower than the tabulated value of chemically pure titanium.

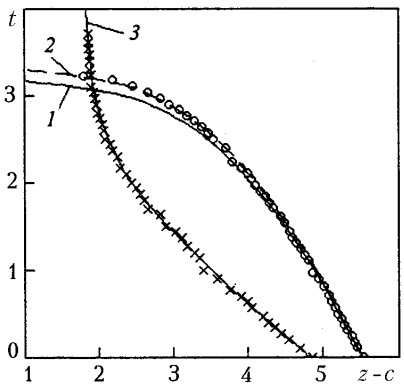

Fig. 4. Results of measurement (points) and calculation (curves) of the position as a function of time for a titanium (1 and 2) and a starch particle (3).

Also, we have investigated the suspension of potato-starch granules in distilled water (no data on the magnetic susceptibility of potato starch were found in the literature). The results of measurement for a granule about 25 μm in size are also presented in Fig. 4. It is seen that, unlike titanium particles, the settling rate of starch granules decreases as the cylinders are approached, suggesting that starch is a diamagnetic with a susceptibility exceeding the diamagnetic susceptibility of the carrier fluid (water) in absolute value. Consequently, we have sign $(\Delta\rho) = 1$ and sign $(\Delta\chi) = -1$ in (6) for the starch granules. Using the measured value of the coordinate of the initial position $z_0 = c + 4.8$, we obtain the best approximation of the measurement results for the value of the free-settling rate $v_0 = 218$ μm/sec and the value of the magnetophoretic parameter $M = 0.86$. The calculation result is presented in Fig. 4 by curve 3 and demonstrates a virtually complete coincidence with experiment. Using $\rho = 1.67$ g/cm^3 for starch, we find $\Delta\chi = -0.153\cdot10^{-6}$. This yields $\chi = -0.87\cdot10^{-6}$ for the magnetic susceptibility of starch.

Conclusions. Noteworthy are certain features of the procedure considered. First, the magnetic susceptibility of a particle is determined from the results of measurement of the integral curve of motion at a fairly long distance and, since the accuracy of video-computer recording of the time and position of the particle is very high, the influence of random errors turns out to be negligible. This is demonstrated by the slight deflection of experimental points in Fig. 4 from the curves. The assumption according to which a particle follows a trajectory that is close to a vertical straight line is directly verified by its picture. Thus, possible errors in determining susceptibility are systematic in character and are associated with the precision of manufacture and assembly of the cell and the accuracy of determination of the saturation magnetization of the cylinder material. Thus, the possible reason why the titanium susceptibility measured varies from its tabulated value is that the saturation magnetization differs from the value adopted in calculations for chemically pure iron. The advantage of the method is that the influence of the fluid viscosity and the particle size and shape is excluded in it. Also, noteworthy is the fact that the method allows measurement of the susceptibility of the particle material when the particle can absorb the carrier fluid and, in doing so, even change its volume, in any case to an extent to which the density and magnetic susceptibility of such a modified particle are additive to the densities and susceptibilities of its components. We show this as follows. In the measured value of the magnetophoretic parameter M, we should use $\Delta\chi_{\text{eff}} = \chi_{\text{eff}} - \chi_0$ instead of $\Delta\chi$ and the dependence $\Delta\rho_{\text{eff}} = \rho_{\text{eff}} - \rho_0$ instead of $\Delta\rho$ in the case in question. Assuming that the effective susceptibility and effective density of the modified particle are determined by the relations

$$\chi_{\text{eff}} = \frac{\chi V_{\text{s.b}} + \chi_0 V_{\text{f}}}{V_{\text{s.b}} + V_{\text{f}}}, \quad \rho_{\text{eff}} = \frac{\rho V_{\text{s.b}} + \rho_0 V_{\text{f}}}{V_{\text{s.b}} + V_{\text{f}}},$$

we find that

$$\frac{\Delta\chi_{\text{eff}}}{\Delta\rho_{\text{eff}}} \equiv \frac{\Delta\chi}{\Delta\rho}.$$

The last expression yields that if particles absorb the carrier fluid, to reconstruct the true magnetic susceptibility of their material from the results of determination of the magnetophoretic parameter M in formula (4) one should take the particle density that has been measured by the pycnometric method with the use of a fluid used in magnetophoretic experiments. It is precisely by such a method that we determined the density of starch grains.

This work was partially financed by the Belarusian Republic Foundation for Basic Research (project T03-204).

NOTATION

B, width of a ferrocylinder, cm; b, dimensionless width of a ferrocylinder; C, half-height of a ferrocylinder, cm; c, dimensionless half-height of a ferrocylinder; d, particle diameter, cm; $\mathbf{e}$, unit vector in the direction of the external magnetic field; $\mathbf{F}_m$, magnetophoretic force, cm·g/sec^2; $\mathbf{f}_m$, dimensionless magnetophoretic force; $\mathbf{H}_0$ and $\mathbf{H}'$, strength of the external magnetic field and the eigenfield of ferrocylinders, Oe; $\mathbf{h}$, dimensionless strength of the magnetic eigenfield of ferrocylinders; I_s, saturation magnetization of ferrocylinders, G; g, free-fall acceleration, cm/sec^2; $\mathbf{i}$, $\mathbf{j}$, and $\mathbf{k}$, unit vectors of the Cartesian coordinate system; L, half-length of the channel, cm; l, dimensionless half-length of the channel; M, dimensionless magnetophoretic potential; P, dimensionless strength of the external magnetic field; $\mathbf{R}$, radius vector of a particle; $\mathbf{r}$, dimensionless radius vector; t, time, sec; X, Y, Z, Cartesian coordinates; x, y, z, dimensionless Cartesian coordinates; x_0, y_0, z_0, coordinates of the initial position of a particle; v_0, rate of free sedimentation of a particle, cm/sec; V, particle volume, cm^3; W, half-width of the channel, cm; α, parameter of shape of a particle; β, γ, and ζ, dimensionless variables; ρ and ρ_0, density of a particle and the fluid, g/cm^3; χ and χ_0, magnetic susceptibility of a particle and the fluid (cgsm); η, viscosity, P; Φ, magnetophoretic potential, g·cm^2/sec^2; φ, dimensionless magnetophoretic potential; ω, dimensionless rate. Subscripts: eff, effective; m, magnetophoretic; 0, initial; s, saturation; s.b, solid body; f, fluid.

REFERENCES

1. C. Latour and H. Kolm, Magnetic separation in water pollution control, *IEEE Trans. Magn.*, **Mag-11**, 1570–1572 (1975).
2. C. G. Owen, High-gradient magnetic separation of erythrocytes, *Biophys. J.*, **22**, 171–178 (1978).
3. G. Maret and K. Dransfeld, Biomolecules and polymers in high steady magnetic fields, in: F. Herlach (Ed.), *Strong and Ultrastrong Magnetic Fields and Their Application* [Russian translation], Mir, Moscow (1988), pp. 180–262.
4. A. V. Sandulyak, *Magnetofiltration Cleaning of Liquids and Gases* [in Russian], Khimiya, Moscow (1988).
5. A. J. Richards, T. E. Thomas, O. S. Roath, et al., Improved high-gradient magnetic separation for the positive selection of human blood mononuclear cells using ordered wire filters, *J. Magnetism Magnetic Mater.*, **122**, 364–366 (1993).
6. N. G. Moshechkov, R. S. Makhlin, A. Yu. Baryshnikov, et al., Development of magnetic separator MSK-1 and immunological sorbent in curing oncological and other diseases, in: *Proc. 10th Jubilee Int. Ples Conf. on Magnetic Fluids* [in Russian], Ples (2002), pp. 343–346.
7. M. Zborowski, G. R. Ostera, L. R. Moor, S. Milliron, J. J. Chalmers, and A. N. Schechter, Red blood cell magnetophoresis, *Biophys. J.*, **84**, 2638–2645 (2003).
8. B. E. Kashevskii and I. V. Prokhorov, Magnetophoretic potential of a chain of ferromagnetic balls in a homogeneous field, *Inzh.-Fiz. Zh.*, **76**, No. 4, 30–35 (2003).
9. B. E. Kashevskii, Magnetophoretic potential of a plane-ordered system of ferrocylinders. 1. Circular cylinders, *Inzh.-Fiz. Zh.*, **76**, No. 6, 70–74 (2003).
10. B. E. Kashevskii, Magnetophoretic potential of a plane-ordered system of ferrocylinders. 2. Rectangular cylinders, *Inzh.-Fiz. Zh.*, **76**, No. 6, 75–79 (2003).
11. B. E. Kashevskii, Magnetophoretic properties of a volume-ordered system of rectangular ferrocylinders, *Inzh.-Fiz. Zh.*, **78**, No. 3, 44–50 (2005).
12. Yu. A. Plyavin' and E. Ya. Blum, Magnetic properties of para- and diamagnetic blood cells in high-gradient magnetic separation, *Magn. Gidrodin.*, No. 4, 3–14 (1983).